Phosphate enrichment induces increased dominance of the parasite *Aquarickettsia* in the coral *Acropora cervicornis*

J. Grace Klinges [1,2,*], Shalvi H. Patel[1], William C. Duke[1], Erinn M. Muller[2,3] and Rebecca L. Vega Thurber[1]

[1]Department of Microbiology, Oregon State University, 226 Nash Hall, Corvallis, OR 97331, USA
[2]Mote Marine Laboratory International Center for Coral Reef Research and Restoration, 24244 Overseas Hwy, Summerland Key, FL 33042, USA
[3]Mote Marine Laboratory, 1600 Ken Thompson Pkwy, Sarasota, FL 34236, USA
*Corresponding author: Mote Marine Laboratory International Center for Coral Reef Research and Restoration, 24244 Overseas Hwy, Summerland Key, FL 33042, USA. Tel: +(941) 504-3801; E-mail: gklinges@mote.org

One sentence summary: Nutrient-enriched nearshore water induced increases in total bacterial abundance over the course of experimentation, but only the addition of phosphate significantly altered the dominance of the parasite Aquarickettsia over other members of the microbiome.
Editor: Julie Olson

Abstract

Nutrient pollution is linked to coral disease susceptibility and severity, but the mechanism behind this effect remains underexplored. A recently identified bacterial species, '*Ca.* Aquarickettsia rohweri,' is hypothesized to parasitize the Caribbean staghorn coral, *Acropora cervicornis*, leading to reduced coral growth and increased disease susceptibility. *Aquarickettsia rohweri* is hypothesized to assimilate host metabolites and ATP and was previously demonstrated to be highly nutrient-responsive. As nutrient enrichment is a pervasive issue in the Caribbean, this study examined the effects of common nutrient pollutants (nitrate, ammonium, and phosphate) on a disease-susceptible genotype of *A. cervicornis*. Microbial diversity was found to decline over the course of the experiment in phosphate-, nitrate-, and combined-treated samples, and quantitative PCR indicated that *Aquarickettsia* abundance increased significantly across all treatments. Only treatments amended with phosphate, however, exhibited a significant shift in *Aquarickettsia* abundance relative to other taxa. Furthermore, corals exposed to phosphate had significantly lower linear extension than untreated or nitrate-treated corals after 3 weeks of nutrient exposure. Together these data suggest that while experimental tank conditions, with an elevated nutrient regime associated with coastal waters, increased total bacterial abundance, only the addition of phosphate significantly altered the ratios of *Aquarickettsia* compared to other members of the microbiome.

Keywords: nutrient enrichment, parasite, coral, differential abundance, absolute abundance, diversity

Introduction

The scleractinian coral holobiont, composed of diverse bacterial, archaeal, viral, and eukaryotic microorganisms, directly and indirectly influences the health, nutrition, and development of the coral organism (Rosenberg et al. 2007, Krediet et al. 2013, Bourne et al. 2016, Webster and Reusch 2017). These taxa perform numerous services for their host including nitrogen fixation, sulfur cycling, and protection against pathogens (Bourne et al. 2016, Glasl et al. 2016). The coral holobiont plays an essential role in coral responses to changing environments and likely mediates host resilience to stress, as environmentally induced changes in microbiome structure are hypothesized to facilitate host adaptation (Bourne et al. 2016, Webster and Reusch 2017). While microbiome responses to short-term stressors (such as thermal stress) may be reversed with the removal of the stressor (Bourne et al. 2008, Ziegler et al. 2019, Maher et al. 2020), cumulative and long-term stressors (such as nutrient enrichment) can shift the coral microbiome from mutualistic to pathogenic (Bourne et al. 2016; McDevitt-Irwin et al. 2017). Different coral species may have different strategies to prevent this shift: while the high microbial diversity harbored by some corals may buffer some negative effects of environmental stress by providing functional redundancy and

the potential for microbiome restructuring, other corals maintain a core microbial repertoire of beneficial species and may possess higher capacity for resisting pathogens (Ziegler et al. 2019).

While the well-documented decline in coral diversity and coverage worldwide (Huang and Roy 2015, Hughes et al. 2017) can primarily be attributed to warming ocean temperatures and coral disease, these stressors are exacerbated by localized and manageable stressors including nutrient pollution (Donovan et al. 2021). These stressors interact to cause changes in coral physiology and microbiome composition that contribute to low stress resilience and high mortality (Zaneveld et al. 2016; Vega Thurber et al. 2012, 2014, Pawlik et al. 2016, Shaver et al. 2017). Corals thrive in oligotrophic tropical water due to their closely managed exchange of nutrients with the endosymbiotic dinoflagellate Symbiodiniaceae, a relationship that depends on low available nitrogen to stimulate highly efficient phosphorus cycling (Wooldridge 2010, Shantz and Burkepile 2014). This symbiosis is disrupted by external N and P inputs from human activities, which are so significant that anthropogenic nutrient input has surpassed natural nutrient sources over the past century (Bennett et al. 2001, Shantz et al. 2016). Field surveys and manipulative experiments alike have suggested that the severity, rapidity, and frequency of coral dis-

eases is also related to local nutrient concentrations (Bruno et al. 2003; Voss and Richardson 2006, Vega Thurber et al. 2014). Further, Vega Thurber et al. (2014) demonstrated that nutrient enrichment increased both the prevalence and severity of disease in enriched corals as well as the prevalence of bleaching, and that after cessation of nutrient exposure, bleaching and disease prevalence returned to baseline levels. Nutrient enrichment induces the overgrowth of macroalgae and turf algae (De'ath and Fabricius 2010, Lapointe and Bedford 2011) with demonstrated negative effects on coral health (Pratte et al. 2018; Vega Thurber et al. 2012).

We previously showed that a common bacterial symbiont of *Acropora cervicornis*, 'Ca. *Aquarickettsia rohweri*', proliferates in response to nutrient-enriched conditions and was strongly associated with reduced coral growth rates (Shaver et al. 2017), and that increased abundances of the order Rickettsiales were associated with increased disease prevalence and tissue loss in other coral species (Table S1 (Supporting Information) of Zaneveld et al. 2016). These putative parasites are hypothesized to influence Acroporid disease susceptibility through the overconsumption of host and symbiont nutritional and energy resources (Klinges et al. 2019). The relationship between *Aquarickettsia* and Caribbean acroporids appears to be long-established, as Rickettsiales-like organisms were found in all histological samples of these coral species since 1975 (Peters et al. 1983, Miller et al. 2014). Despite this, *Aquarickettsia* does not appear to coevolve with its coral host, but rather varies phylogenetically by geographic region, suggesting that this species is highly environmentally responsive (Baker et al. 2021).

The primary nutrient inputs to oligotrophic reef systems, nitrogen (as nitrate and ammonium) and phosphorus, each have distinct effects on coral physiology. Importantly, anthropogenic nutrification of these systems often leads to not only an increase in these constituents but also an alteration of the ratio between their concentrations (Brodie et al. 2011, Wiedenmann et al. 2013). As nutrient enrichment has become more pervasive in reef environments and often co-occurs with other stressors, disentangling the effects of individual stressors *in situ* is complex. We conducted a manipulative 6-week nutrient enrichment experiment in aquaria, allowing us to examine impacts of individual chemical constituents of nutrient pollution, specifically ammonium, phosphate, and nitrate in isolation and in concert, on the coral microbiome and coral health. To measure changes in key members of the *A. cervicornis* microbiome we used four different abundance metrics: relative abundance (% of total microbial community) from 16S amplicon data, quantitative PCR of a gene specific to the dominant taxon *Aquarickettsia*, analyses of differential abundance (shifts in abundance of individual taxa compared to other taxa) using ANCOM-II, and beta-binomial regressions using the R package corncob to model differential abundance of individual ASVs. We found that while phosphate enrichment stimulated an increase in the coral-associated parasite *Aquarickettsia* relative to other taxa, all forms of nutrient enrichment led to an increase in total bacterial abundance such that measured absolute abundance of *Aquarickettsia* increased significantly but these changes were found to be insignificant when examined using differential abundance metrics.

Materials and methods
Nutrient enrichment experiment

To test the individual and combined effects of different forms of nutrient enrichment on *Aquarickettsia* populations and coral health, a 6-week tank experiment (Figure S1, Supporting Infor-

mation) was conducted at the Mote Marine Laboratory International Center for Coral Reef Research & Restoration (24°39 41.9 N 81°27 15.5 W) in Summerland Key, Florida. The experiment was conducted from April to June 2019 in 40 independent 4.7 l flow-through, temperature-controlled aquaria with natural locally sourced sea water from the Atlantic side of the Keys. Sand- and particle-filtered water was fed from header tanks to aquaria by powerheads fitted with tubing splitters (two tanks per powerhead) at a flow rate of 256.66 ± 43.89 ml/min. Aquaria were located outdoors under natural light regimes with the addition of 75% shade cloth to account for shallow aquarium depth. Aquaria were divided between two flow-through seawater raceways (20 aquaria per raceway), which allowed for temperature regulation of individual aquaria. Raceway water was prevented from entering aquaria by maintaining water levels below in and outflow holes using a standpipe. Water temperatures were maintained at an average of $27.19 \pm 0.6°C$. Temperature was controlled by a boiler and chiller using a dual heat exchanger system connected to header tanks and individual raceways. Header tank pH was stabilized at ∼8.0 by aeration and mixed via a venturi pump system. Nutrient levels in aquaria were elevated compared to conditions at the coral collection site (Mote Marine Laboratory's *in situ* coral nursery in Looe Key) as intake pipes were located in coastal water instead of offshore reef water (Figure S1, Supporting Information). While ammonium and phosphate levels were similar to reef conditions, nitrate concentration was 4-fold higher in aquaria compared to Looe Key. Aquaria were cleaned every third day to prevent overgrowth of coral fragments with diatoms or algae.

A total of 180 fragments (∼5 cm) were collected from *A. cervicornis* genotype 50 in the Mote Marine Laboratory *in situ* coral nursery in Looe Key in April 2019. This genotype was previously delineated *via* microsatellite genotyping and was found to have a high level of disease susceptibility (Muller et al. 2018, Klinges et al. 2020). Genotype 50 is known to host *Symbiodinium fitti*, the primary species of Symbiodiniaceae found in the Mote *A. cervicornis* nursery corals (Muller et al. 2018, Parkinson et al. 2018). A total of six fragments were housed in each aquarium. Prior to experimental manipulation, fragments were allowed to acclimate to aquarium conditions for 7 days. After acclimation, each aquarium was assigned one of nine nutrient treatments (Figure S1, Supporting Information). Aquaria were exposed to elevated levels of each nitrate (in the form of $NaNO_3$), ammonium (as NH_4Cl), phosphate (as Na_3PO_4), a combination of the three, or a no-treatment control. Nutrient levels were elevated to approximately 3x and 4x unamended aquarium conditions (Figure S1, Supporting Information). For 42 days (6 weeks), each enriched tank was spiked with nutrient treatment four times a day (every 6 h). Flow in all aquaria was stopped for an hour immediately following the nutrient additions. This resulted in an hour-long nutrient pulse four times a day, followed by 1 h of dilution and 4 h at ambient concentration. Nutrient treatments were randomly distributed across raceways, with each raceway containing all nutrient treatments and untreated tanks. Coral total linear extension (TLE) was assessed by measuring fragments at their longest point initially and biweekly thereafter. Due to the skewed nature of the TLE data, data were log-transformed before a Tukey's Honest Significance test was used to compare differences in TLE by nutrient treatment. Rough assessments of algal symbiont concentrations and coral health were made using a Coral Watch Coral Health Chart (Siebeck et al. 2008). The CoralWatch Coral Health Chart provides a 6-point scale with which changes in coral color can be measured as an indicator of symbiont density. Photographs of each coral individual were taken contemporaneously with coral health card measurements. A total of 18 fragments were lost over the course of the experiment.

Sample collection and preservation

A total of 166 coral fragments were sampled at three time points throughout the experiment: prior to nutrient exposure (T0), after 3 weeks, and after 6 weeks. Fragments were sampled immediately after removal from aquaria, and fragments were sacrificed (i.e. not returned to aquaria) after sampling. Once removed from the tank, tissue was scraped from one side of each fragment (avoiding the apical tip) using sterile bone cutters and added directly to 2 ml tubes containing 1 ml DNA/RNA shield (Zymo Research) and Lysing Matrix A (MP Biomedicals, 0.5 g garnet matrix and one 1/4" ceramic sphere). Tubes were immediately preserved at −80°C until further processing. Total DNA was extracted from 500 μl of tissue slurry using the E.Z.N.A.® DNA/RNA Isolation Kit (Omega Bio-Tek) and was stored at −80°C until preparation for sequencing. DNA yield from a total of 12 samples was found to be insufficient for sequencing.

Nutrient analyses using an Autoanalyzer were performed to confirm that aquaria received the expected nutrient dose. Samples were collected using acid washed (10% HCl with DI rinse) syringes with BD Luer-Lok™ tips and filtered using combusted GFF filters (fired in a muffle furnace at 500°C for 1.5 h) housed in acid-washed polypropylene filter holders (MilliporeSigma). Samples were frozen overnight at −80°C and shipped overnight on ice to Mote Marine Laboratory in Sarasota, FL. Samples were processed on a 3-channel AA3 HR Autoanalyzer (Seal Analytical, Southampton, UK).

Quantitative polymerase chain reaction protocols and analysis

To track absolute abundance of *Aquarickettsia*, quantitative polymerase chain reaction (qPCR) was performed on 153 samples (each in triplicate) using primers designed to target the *A. cervicornis* actin gene (as an endogenous control, Wright et al. 2018) and an *Aquarickettsia*-specific gene, ATP/ADP translocase *tlc1* (Baker et al. 2021), using iQ SYBR Green Supermix (Bio-Rad, Hercules, CA). An 149 bp section of the *tlc1* gene of *A. rohweri* was amplified in 20 μl reactions using sequence-specific primers at 0.3 μM (F: 5′-GGCACCTATTGTAGTTGCGG-3′, R: 5′-CATCAGCTGCTGCCT TACCT-3′). The *tlc1* gene of *A. rohweri* was previously found to be distinct from annotated *tlc1* genes in related Rickettsiales species, with only 51% amino acid identity to the *tlc1* gene of 'Ca. Jidaibacter acanthamoeba,' from within the same family ('Ca. Midichloriaceae'; Klinges et al. 2019; Table S1, Supporting Information). The amino acid sequences of the *tlc1* genes of two recently sequenced strains of *A. rohweri* were found to be 99.76% and 73.18% identical to the *tlc1* amino acid sequence of *A. rohweri*, strain Acer-44 (Figure S2 and Table S1, Supporting Information). The resultant amplicon size produced by our specific tlc primer pair was confirmed through endpoint PCR of the *tlc1* and 16S rRNA genes (updated 515F-806R primer set, Apprill et al. 2015, Parada et al. 2016) using AccuStart™ II PCR ToughMix (QuantaBio, Beverly, MA) and subsequent gel electrophoresis on a 1.5% agarose gel with Invitrogen 100 bp DNA Ladder (ThermoFisher Scientific, Waltham, MA). A single amplicon was confirmed to be produced in *A. cervicornis* genotype 50 samples by the *tlc1* primer set, with 16S primers used as a positive control, and no product was produced by our *tlc1* primer pair using *Pseudomonas aeruginosa* strain PAO1 as a template (Figure S3, Supporting Information). The actin gene of *A. cervicornis* was amplified as in Wright et al. (2019) as an endogenous control. A sample of *Acropora hyacinthus* (collected from Moorea, French Polynesia in 2017) was used as a calibrator, as this species expresses actin but lacks *A. rohweri*. A positive control (a sample of adult genotype 50 with high abundance of *A. rohweri*, used across all runs) and a no-template control (molecular grade water) were prepared using the same methods and quantified simultaneously. A 35-cycle qPCR was performed on an Applied Biosystems 7500 Fast Real-Time PCR System, using cycling parameters selected to minimize mispriming: An initial denaturation step of 3 min at 95°C, followed by 35 cycles of 95°C for 15 s, 56°C for 30 s, and 72°C for 30 s. Melt curve analysis was performed to identify any off-target products and Relative quantitation (RQ) methods were used to assess fold change of *tlc1*. Melt curves (Figure S4, Supporting Information) reveal a single peak (T_M) at 78.4°C for the *tlc1* amplicon, and a single peak at 83.9°C for the actin amplicon. The baseline fluorescence of *tlc1* and actin was adjusted for each run such that threshold cycle (Ct) values of the calibrator sample fell within an ±0.5 range. Outliers (outside 1.5x interquartile Ct range) were removed before calculating the average Ct value (Jian et al. 2020). Only runs with no amplification in the NTC were kept. RQ determines the change in expression of the target sequence (*tlc1*) in tested samples relative to the same sequence in the calibrator sample (*Ac. hyacinthus*). RQ results were reported as average relative expression ($\Delta\Delta$Ct, expression of samples compared to calibrator) with an associated 95% confidence interval. Due to the nonparametric nature of the data, differences in expression between samples were analyzed using a Kruskal–Wallis rank sum test with Dunn's test for multiple comparisons, using the Benjamini–Hochberg method to adjust P value for multiple comparisons. RQ values were log-transformed for temporal comparison.

Polymerase chain reaction and sequencing protocols

The bacterial community dynamics of each of 157 coral samples was analyzed using 16S rRNA Illumina sequencing on the MiSeq platform. The V4 region of the 16S rRNA gene was amplified *via* 2-step polymerase chain reaction (PCR) utilizing forward and reverse primers 515F (5′-GTG YCA GCM GCC GCG GTA A-3′; Parada et al. 2016) and 806R (5′-GGA CTA CNV GGG TWT CTA AT-3′; Apprill et al. 2015). First-step reactions (12.5 μl reaction volume) were performed using 6.25 μl AccuStart II PCR ToughMix (2X, Quantabio), 1.25 μl forward primer (10 mM), 1.25 μl reverse primer (10 mM), 0.5 μl sample DNA, and 3.25 μl PCR-grade water. PCR was performed with a 3 min denaturation at 94°C; 35 cycles of 45 s at 94°C, 60 s at 50°C, and 90 s at 72°C; followed by a final elongation step at 72°C for 10 min and a 4°C hold. To avoid host DNA contamination, amplified samples were run on a 1.5% low melting point agarose gel until ∼1 cm separation was achieved between the off-target 12S rRNA host band and target product 16S rRNA band. Second-step PCR was conducted according to the methods described in Ezzat et al. (2021) and Messyasz et al. (2021). Each visible 16S band was poked with a sterile 10 μl plastic pipette tip, which was swirled into a barcoding master mix solution containing 12.5 μl AccuStart II ToughMix (2X), 9.5 μl PCR-grade water, and 1 μl (10 mM) each of custom forward and reverse barcodes (dual indices with custom adapters). The 12-cycle PCR reaction consisted of a 5 min denaturation step at 95°C, 30 s melting at 95°C, 3 min annealing at 63°C, 30 s extension at 72°C, and 10 min hold at 72°C. Barcoded products were purified using Agencourt® AMPure XP beads (Beckman Coulter, CA) and dsDNA quantified using an Invitrogen Qubit 4 Fluorometer (ThermoFisher). Samples were then pooled together in equimolar proportions based on their molecular weight and DNA concentrations. Libraries were sequenced at Oregon State University's Center for Genome Research and Bio-

computing (CGRB) Core Laboratories on an Illumina MiSeq sequencing platform, 2×300 bp version 3 chemistry according to the manufacturer's specifications.

Amplicon sequencing bioinformatic and statistical analysisQuality control and filtration

Demultiplexing and barcode removal was performed using cutadapt (Martin 2011), during which reads with no barcode match were discarded. A total of 6 623 631 reads across 153 samples (average depth of 43 011 reads/sample) were subsequently processed using DADA2 (Callahan et al. 2016) in R (version 4.0.3, R Development Core Team 2019). Based on quality plots, forward and reverse reads were truncated at their 3′ end at 250 and 200 base pairs, respectively. Sequences were truncated at the first position having a quality score less than or equal to 10, and reads with a total expected error of > 2 or with the presence of Ns were discarded, resulting in a total of 3 517 216 reads. A total of three samples were removed that sequenced poorly, with a read depth of less than 30 reads after quality control. An initial total of 1948 amplicon sequence variants (ASVs) were inferred from unique reads and paired-end reads were subsequently merged. ASVs that did not match a target length of 250 ± 4 (73 ASVs) were discarded. A total of 228 two-parent chimeras (bimeras) were removed (equating to 68 101 reads) and taxonomy was assigned at 100% sequence identity using the Silva reference database (v132.1) in order to preserve the high resolution of ASV data (Quast et al. 2012). The resulting ASV table contained 1647 unique ASVs across 150 samples (Table S2, Supporting Information) and was imported into *phyloseq* (v1.30.0; McMurdie and Holmes 2013). A total of 99 ASVs were then removed from the dataset that were annotated as mitochondrial, chloroplast, or eukaryotic sequences, corresponding to a total of 119 995 reads, leaving a total of 1548 ASVs. After processing in *phyloseq*, the Silva taxonomic classification for the genus MD3-55 was changed to *Ca*. Aquarickettsia in accordance with current identification in the literature (Klinges et al. 2019). Additionally, ASVs classified only to a certain taxonomic level (e.g. annotated only to the family level) were renamed at lower taxonomic levels to reflect the lowest annotated level (e.g. unknown genus in family *Francisellaceae* renamed at genus level to 'Family *Francisellaceae*').

Alpha diversity analyses using unpruned, rarefied data

Using alpha rarefaction curves in *phyloseq*, the sequence table (1548 ASVs) was rarefied to a minimum sequence depth of 5098 reads, which sufficiently included all samples while still maximizing sample diversity, with a total of 1259 ASVs retained. This dataset was subsequently used for alpha diversity analyses. Differences observed in Simpson's diversity index (Heip et al. 2001) between groups (groups exposed to different nutrient treatments, different levels of individual nutrients, and different periods of exposure) were tested with the Pairwise Wilcoxon Rank Sum Test with FDR correction for multiple testing. To determine the dynamics of minor taxa in the community, alpha diversity analyses were repeated after removal of *Aquarickettsia* sequences, which reduced sequencing depth such that a new rarefaction level of 351 reads/sample was used.

Beta diversity analyses using pruned data

ASVs with a total count across the dataset in the bottom first-quartile (count ≤ 5) were pruned resulting in a total of 3 285 137

total reads with a median sample depth of 21 377 reads. This equated to a removal of only 1611 reads across the dataset and 479 ASVs. After quality control and pruning, a total of 1069 ASVs remained in the dataset (frequency per ASV: median = 20, mean = 3072, min = 6, and max = 2 456 404). Although there were no singletons in the dataset, 580 ASVs (corresponding to 12 251 reads) were present in only one sample each in the final dataset.

The pruned, unrarefied ASV table was centered log-ratio (CLR) transformed for beta diversity analyses using the tool 'clr' from the microbiome package (Lahti and Shetty 2012) as was an unrarefied ASV table with *Aquarickettsia* sequences removed. Principal components analysis (PCA) was performed using Euclidean distances calculated from the CLR-transformed dataset with the phyloseq command ordinate (as RDA without constraints). Ordinations identified one sample as an outlier, which was subsequently removed. Permutational Multivariate Analysis of Variance (PERMANOVA; Anderson 2001) was performed on calculated Euclidean distances to test for differences in beta diversity of the bacterial community compositions among groups exposed to different nutrient treatments, different levels of individual nutrients, and different periods of exposure. PERMANOVA was performed using the function adonis from the package vegan (v2.5.5) (Oksanen et al. 2019) and was followed by pairwise analysis of variance with pairwiseAdonis (v0.01; Martinez Arbizu 2017) using Euclidean distance and 999 permutations. Permutational Analysis of Multivariate Dispersions (PERMDISP; Anderson 2006) was performed to examine shifts in multivariate dispersion over time and between groups using the function betadisper and pairwise analysis was performed using the function permutest with FDR adjusted *P*-values (both in vegan v2.5.5, Oksanen et al. 2019). Differences in relative abundance observed between treatment groups and by exposure weeks were assessed by Kruskal–Wallis chi-squared test and the Pairwise Wilcoxon Rank Sum Test with FDR correction for multiple testing.

An Analysis of Composition of Microbiomes (ANCOM-II, v2.1, Kaul et al. 2017) was performed to identify taxa that were differentially abundant by treatment group. The unrarefied, pruned ASV table was first subset to contain only taxa with at least 10 counts in 20% of samples and summarized to the genus level with the *tax_glom* command in *phyloseq*. This resulted in a table with 29 genera by 150 samples with a median sequencing depth of 21 206. ANCOM v2.1 is a compositionality-aware test that uses a CLR transformation to compare mean relative abundance of taxa between groups with consideration of the zeros in the data (Kaul et al. 2017). Outlier zeros, identified by finding outliers in the distribution of taxon counts within each sample grouping, were ignored during differential abundance analysis and replaced with NA, while structural zeros (absent in one grouping but present in the other) were automatically called as differentially abundant. We selected a significance level at $W = 0.8$ in which the null-hypothesis for a given taxon was rejected in 80% of the tests and *P*-values were corrected with Benjamini–Hochberg FDR (Benjamini and Hochberg 1995, Kaul et al. 2017). One model was run for each of several pairwise contrasts between combinations: Untreated samples vs. T0, nutrient (all nutrient treatments pooled) vs. T0, and each individual treatment vs. T0. Tank identity was included in each model as a random effect. Analysis with corncob (v0.20, Martin et al. 2020) was performed on the unrarefied, unpruned dataset to contrast with ANCOM-II analysis and identify coefficients of response in ASV abundance and variability to nutrient treatment (see Supplemental methods).

Results

Microbiomes of disease-susceptible *A. cervicornis* dominated by *Aquarickettsia* and unclassified taxa

The microbiomes of all samples of *A. cervicornis* used in this study were dominated by the bacterial genus *Aquarickettsia*, with a mean relative abundance of 74.98% ± 17.09% (Fig. 1). Importantly, our methodology utilizing DADA2 retained the unique sequence identity of each sequence variant, allowing us to ascertain that although a total of six sequence variants of the species *A. rohweri* were observed, only one variant was dominant, with all others averaging less than 1% relative abundance across the dataset. Other highly represented taxa included two separate unclassified Proteobacteria (ASV2, 5.934% ± 7.081% relative abundance and ASV6, 1.144% ± 2.482% relative abundance), as well as single variants from the genus *Spirochaeta* (3.526 ± 2.727%) and the families *Francisellaceae* (1.538% ± 3.117%) and *Helicobacteraceae* (0.770% ± 1.720%).

Nucleotide BLAST was used to query the NBCI nr/nt (nonredundant nucleotide) database for the sequences classified as 'unclassified Proteobacteria.' The top four results for the more abundant unclassified Proteobacteria (ASV2) were from samples collected from *A. cervicornis* or *palmata* with % identity ranging from 100% to 98.46%, suggesting that this taxon may be common in Acroporid corals. All other BLAST results had a % identity below 90%. Top BLAST results from the less abundant (ASV6) unclassified taxon were from diverse marine environments ranging from the gill of a chiton in Vanuatu and a hypersaline region of the Mediterranean, but support classification of this sequence as a Deltaproteobacteria. The abundant ASV from the family Francisellaceae was found to be 100% identical to the NCBI sequence for *Cysteiniphilum litorale* (KX817994), cultured and described by Liu et al. (2017) from seawater samples from southern China. The ASV classified as *Spirochaeta* was most closely related to a strain identified in deep-sea volcanic sediment (HQ588391, Pachiadaki et al. 2011). The sequence from *Helicobacteraceae* was identical to two sequences (GU117961 and GU117962) from *A. cervicornis* samples in Panama (Sunagawa et al. 2010) as well as a sequence from the Caribbean coral *Montastraea annularis* exhibiting signs of white plague (AF544892, Pantos et al. 2003). Sequenced PCR negatives were dominated by the genus *Anaerococcus* (order Clostridiales) and the family Corynebacteriaceae.

Exposure to tank conditions altered microbiomes across all treatments

Of the 150 samples that were successfully sequenced and surpassed quality control thresholds, replication by treatment varied due to survival and sequencing success, with a minimum of 4 corals/treatment and timepoint, and a maximum of 10 (Table S2, Supporting Information). Nutrient analyses confirmed that experimental aquaria received enriched (3x or 4x ambient) levels of either nitrate (in the form of $NaNO_3$), ammonium (as NH_4Cl), phosphate (as Na_3PO_4), a combination of the three, or a no-treatment control (Figure S1, Supporting Information). However, these analyses also indicated that baseline nitrate levels in all aquaria were considerably elevated compared to *in situ* measurements taken in 2014 of coral collection region (Looe Key; Figure S1, Supporting Information). Ammonium concentrations were only slightly elevated in aquaria compared to 2014 Looe Key data and phosphate levels were within 0.01 μM of 2014 data.

Regardless of treatment (Figure S1, Supporting Information), alpha diversity decreased with time after initial introduction to the experimental tank system (Fig. 2). Significant differences in microbial alpha diversity were found between samples collected at time point 0 (T0, no nutrient exposure), and samples collected at subsequent timepoints (both Simpson's and Shannon's metrics, Pairwise Wilcoxon Rank Sum Test with FDR correction). Pairwise comparisons using both Simpson's and Shannon's metrics of diversity indicated a significant decrease in species richness and evenness between weeks 0 and 3 and between weeks 0 and 6 ($P < .001$, Pairwise Wilcoxon Rank Sum Test with FDR correction, $\chi^2 = 74.851$ (Simpson's), $\chi^2 = 82.812$ (Shannon's)). Differences in Simpson's and Shannon's diversity between weeks 3 and 6 were not significant ($P > .05$), suggesting that microbial communities reached a new stable state with time and 3 weeks of nutrient exposure was sufficient to alter community structure. Tests for differences in Simpson's diversity between individual treatments showed that treatment with ammonium did not induce significant shifts in alpha diversity over time (Fig. 2), and though untreated corals experienced a significant shift after 3 weeks in the experimental system, after 6 weeks in the system, alpha diversity was no longer significantly different from time point 0 (Fig. 2A; Table S3, Supporting Information). Exposure to phosphate, nitrate, and combined treatments shifted alpha diversity by 3 weeks, and diversity remained significantly different from T0 through 6 weeks of exposure.

As the evident dominance of the genus *Aquarickettsia* across all samples was likely to mask shifts in minor taxa, alpha diversity analyses were repeated with *Aquarickettsia* removed from the dataset (which resulted in a new rarefaction depth of 351). The removal of *Aquarickettsia* reduced differences in Simpson's diversity over the course of the experiment across the majority of treatments (Figure S5, Supporting Information). Though overall, alpha diversity decreased with time, only the combined treatment (combination of NO_3, NH_4, and PO_4) exhibited a significant ($P < .001$) decline in Simpson's diversity between weeks 0 and 3 and 0 and 6 after the removal of *Aquarickettsia*. Phosphate treatment induced a significant decrease in alpha diversity with 3 weeks of exposure, but by 6 weeks of exposure, Simpson's diversity was no longer significantly different from T0. Differences between weeks 3 and 6 were not significant for any individual treatment.

Beta diversity analyses on CLR-transformed data showed that the interaction of nutrient treatment and exposure weeks produced distinct microbial communities (PERMANOVA; $P < .001$, $R^2 = 0.18\,012$). Microbial communities of samples from time point 0 were distinct from all other time points regardless of treatment, except for samples under no treatment conditions for 3 or 6 weeks (pairwise PERMANOVA with FDR correction, $P < .01$; Table S4, Supporting Information). PCA using Euclidean distance showed a clear separation between samples from time point 0 and all other timepoints (Fig. 2B), and a lack of distinction between samples of all treatments regardless of duration of exposure, although samples from 3 weeks of untreated conditions were more similar to timepoint zero samples than to other untreated samples. No pairwise comparison between treatments was significant besides comparisons with T0 (e.g. T0 vs. Nitrate; pairwise PERMANOVA with FDR correction, $P < .01$; Table S5, Supporting Information). Pairwise comparisons within treatment by exposure time identified no significant difference between 3 and 6 weeks of exposure to any treatment. Differences in beta diversity between high and low levels of nutrient enrichment across all treatments were not significant, though both levels were significantly different from no nutrient exposure (pairwise PERMANOVA with FDR correction, $P < .01$; Table S6, Supporting Information).

Dispersion visibly declined over the duration of nutrient exposure as well as in untreated corals (Figure S6, Supporting Informa-
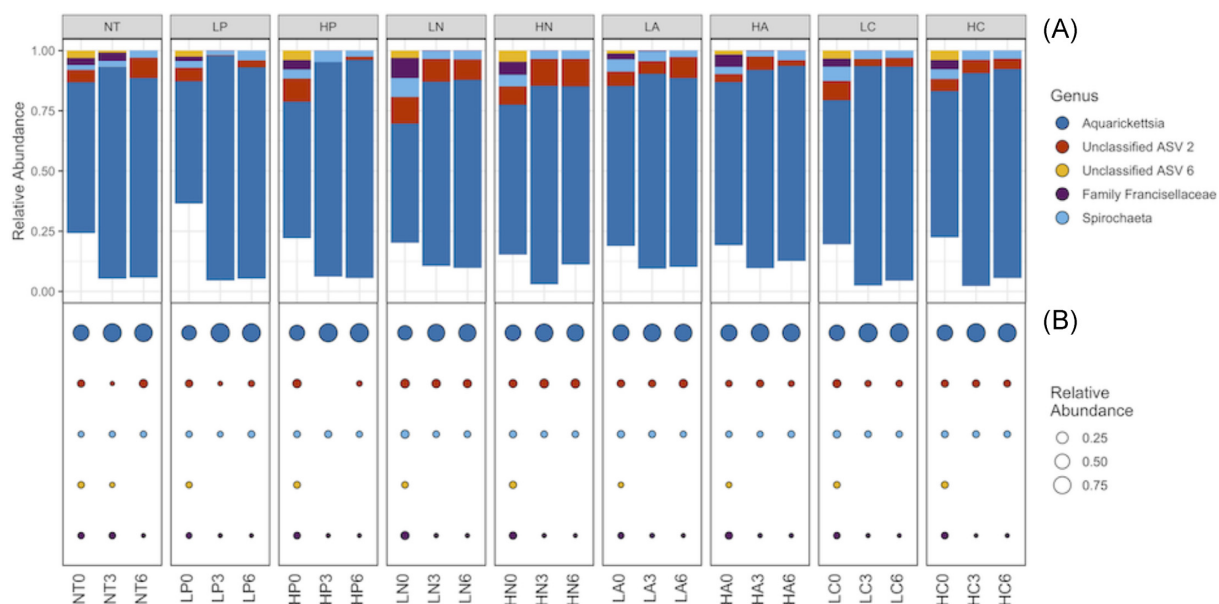
Figure 1. Mean relative abundance of the most abundant genera across three time points in coral fragments exposed to different nutrient constituents. **(A)** Barplot, showing dominance of *Aquarickettsia* across all samples. Taxa are included in the plot if they had a relative abundance greater than 1% across the entire dataset. Each bar represents a minimum of three replicates. **(B)** Bubble plot, showing changes in top five taxa across treatment groups and timepoints. NT = no treatment, L = low (3x ambient), H = high (4x ambient), P = phosphate, N = nitrate, A = ammonium, and C = combined (P, N, and A).
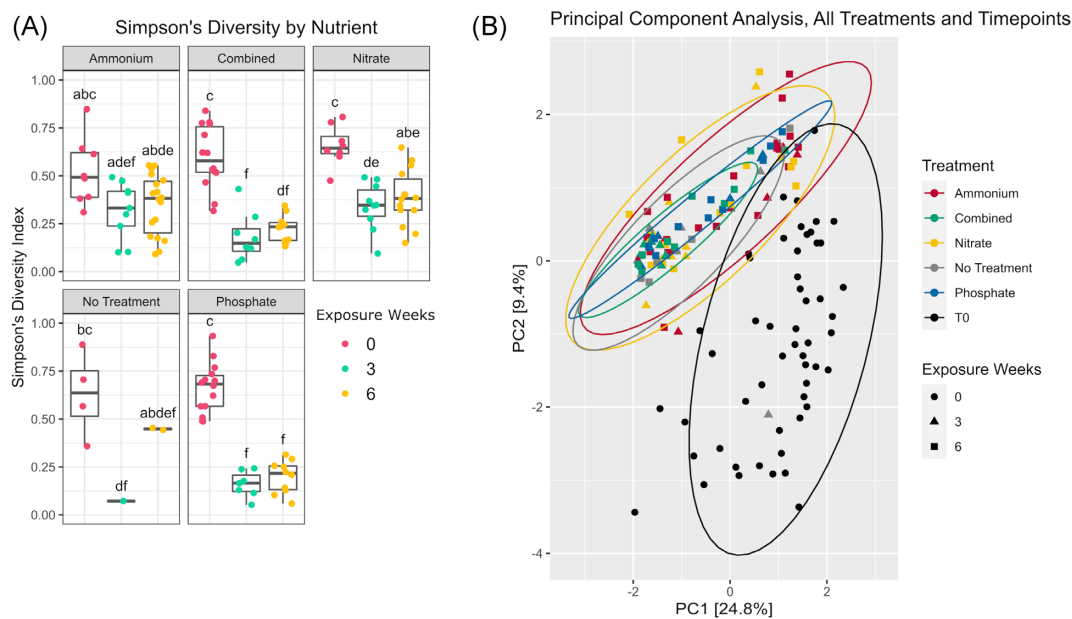
Figure 2. Community diversity metrics by treatment (Ammonium, Combined, Nitrate, Phosphate, or no treatment) and exposure weeks (0, 3, and 6). **(A)**. Simpson's diversity index. Boxes sharing a letter are not significantly different from each other using an FDR corrected significance level of $P < .05$. **(B)**. PCA ordination of samples using Euclidean distance on CLR-transformed data.

tion). Tests for differences in group dispersion, however, showed that decreases in dispersion were only significant in phosphate-treated samples, which experienced a consistent decline between 0 and 6 weeks of exposure, and samples exposed to a combined treatment, which decreased in dispersion significantly after only 3 weeks of exposure ($P < .01$, F = 4.2642). When analyses were repeated on the dataset with *Aquarickettsia* removed (Figure S7, Supporting Information), the significance of this change was lost entirely.

Relative and absolute abundance metrics show increase in *Aquarickettsia* over time

The increase in the dominant taxon *Aquarickettsia* was examined using both relative abundance metrics from amplicon sequencing data and measurements of absolute abundance from quantitative PCR (Fig. 3). According to measures of mean relative abundance, all treatments including untreated tank conditions increased the abundance of *Aquarickettsia*. Differences in relative abundance observed between treatment groups and by exposure
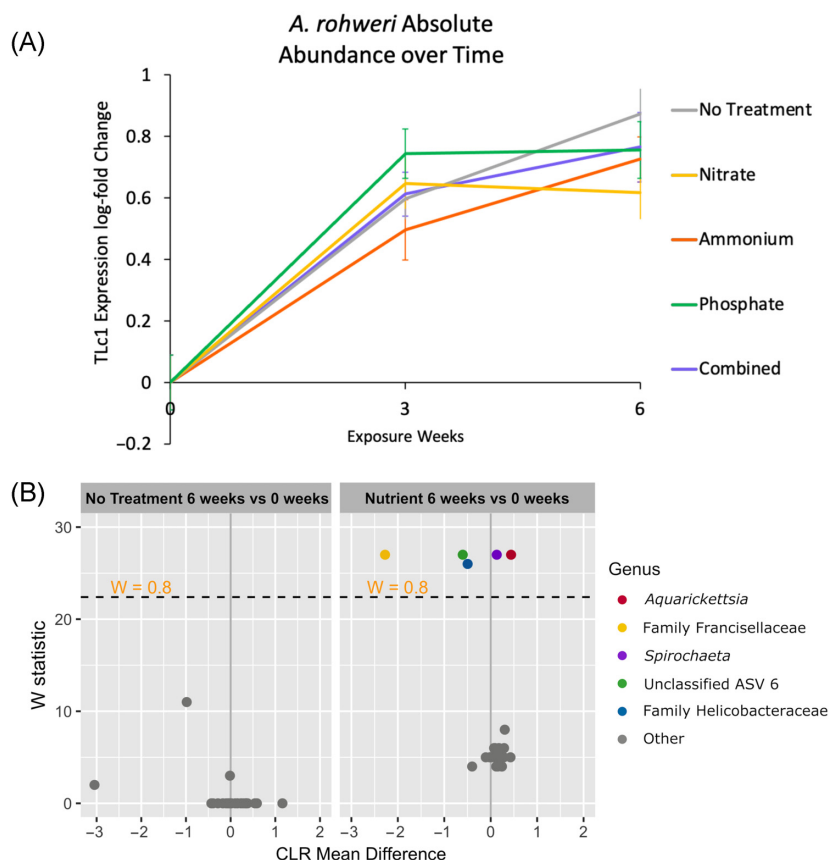
Figure 3. (A). Log-transformed absolute abundance of *A. rohweri* as determined by quantitative PCR. Samples exposed to high and low concentrations of each nutrient were pooled for analysis. The average log-transformed RQ of all timepoint zero samples ($n = 62$) was subtracted from log-transformed RQ of samples at weeks 3 and 6 to assess change in absolute abundance over time. **(B)**. Volcano plot of results from differential abundance analysis with ANCOM-II. Analysis performed on genus-level ASV table was filtered to include taxa with a total count of 10 in at least 20% of samples (ntaxa = 29) was used. ANCOM tests the null-hypothesis that the average abundance of a given species in a group is equal to that in the other group. Contrasts were performed within full ASV table subset to either only no treatment samples, or all other treatments pooled together. The W statistic represents the strength of the test for the 29 tested species and is the number of times the null-hypothesis was rejected for a given species. Taxa above the dashed line are significant with the null-hypothesis rejected 80% of the time (W = 0.8). Nonsignificant taxa in any contrast are colored grey. The *x*-axis value presents the effect size as the CLR-transformed mean difference in abundance of a given species between the two groups being compared. For the second panel, a positive *x*-axis value means the genus was more abundant at 6 weeks of nutrient treatment compared to 0 weeks or *vice versa* for a negative *x*-axis value.

weeks were assessed by Kruskal–Wallis chi-squared test and the Pairwise Wilcoxon Rank Sum Test with FDR correction for multiple testing. *Aquarickettsia* mean relative abundance across treatments at T0 was 58.87 ± 16.26%, and increased significantly ($P < .05$) by 3 weeks of exposure to any treatment to an average of 85.36 ± 9.561%, equivalent to a ~1.46-fold increase in this species. Differences in mean relative abundance of *Aquarickettsia* were not found to be significant between 3 and 6 weeks of exposure, and in fact, relative abundance was found to decline slightly in all treatments from 3 to 6 weeks.

While increases in *Aquarickettsia* relative abundance were significant over time in all treatments, differences in relative abundance among untreated corals and other treatments were not found to be significant at any time point. Significant differences in relative abundance ($P < .05$) were found, however, between phosphate-treated corals and nitrate-treated corals, both at 3 and 6 weeks, and phosphate- and ammonium-treated corals at 6 weeks. *Aquarickettsia* relative abundance increased the most in the phosphate treatment compared to other treatments, reaching peak relative abundance by only 3 weeks of phosphate exposure (Fig. 1). Phosphate-treated individuals had the lowest relative abundance of *Aquarickettsia* at T0, with a % abundance of 53.30 ±

17.63%, and the highest relative abundance of *Aquarickettsia* at week 3, with a % abundance of 91.50 ± 3.758%, as well as the highest at 6 weeks with a % abundance of 89.30 ± 4.814%. Nitrate-treated samples had the lowest relative abundance of *Aquarickettsia* at both 3 (79.59 ± 8.970%) and 6 weeks (76.25 ± 10.97%) compared to other treatments.

In agreement with the relative abundance analysis, measures of change in absolute abundance of *Aquarickettsia* calculated from qPCR data indicated that in all treatments, including untreated tank conditions, the absolute abundance of the parasite *Aquarickettsia* increased. The mean change in absolute abundance was equivalent to a 3.3-fold increase in *Aquarickettsia* over the course of 6 weeks. Phosphate treatment was associated with the greatest change in absolute abundance of *Aquarickettsia* over 3 weeks (average RQ increasing from 191.65 to 1549.81 by week 3) though average RQ values for untreated samples did exceed those from the phosphate treatment by week 6. Untreated samples had the highest ending abundance of *Aquarickettsia* and experienced the greatest magnitude of change across the duration of the experiment (Fig. 3A, average RQ increasing from 290.4 to 1973.4 over 6 weeks, equivalent to a 6.795-fold increase). Pairwise Kruskal–Wallis tests indicated that while all treatments except ammonium exhibited

significant increases ($P < .05$) in *Aquarickettsia* abundance by week 3, no treatment group had a significantly different abundance of *Aquarickettsia* by week 6 ($P > .05$). All changes in abundance between weeks 3 and 6 were insignificant.

Differential abundance metrics reveal that *Aquarickettsia* responded positively to enriched phosphate, while minor taxa responded negatively to other nutrient constituents

Shifts in individual taxa over the course of the experiment were examined using differential abundance analysis of 16S data with the tool 'ANCOM-II' (Figs 3B and 4). Interestingly, although changes in abundance of *Aquarickettsia* were apparent from analysis of absolute abundance data, significant shifts in *Aquarickettsia* were not identified in untreated corals at either 3 or 6 weeks when compared to 0 weeks (Figure S8, Supporting Information). Indeed, there were no significant shifts in any individual taxon in untreated corals over the duration of the experiment (Fig. 3B). Importantly, ANCOM-II presents an analysis of changes in taxon relative abundance in comparison to the geometric mean of taxa in a given group. Thus, while untreated conditions were associated with an increase in absolute abundance of *Aquarickettsia*, this taxon did not increase more than the average change experienced by all taxa in those samples. In contrast, exposure to nutrient treatment was associated with shifts in numerous taxa, including *Aquarickettsia*, across the course of the experiment (Fig. 3B). Analyses of all nutrient treatments pooled together show that while the genera *Aquarickettsia* and *Spirochaeta* responded positively to nutrient enrichment, abundance of sequence variants from the families *Helicobacteraceae* and *Francisellaceae* (*C. litorale,* Liu et al. 2017) as well as an unclassified species (ASV6) declined with nutrient enrichment. Comparisons isolating each nutrient treatment individually showed that increases in *Aquarickettsia* were only significant in phosphate and combined treatments (Fig. 4C and D). When nutrient treatments were examined individually, *Spirochaeta* did not increase significantly in any individual treatment and in fact, was found to decline with the combined treatment. The loss of *Helicobacteraceae, Francisellaceae*, and ASV6 appeared to be driven by nitrate enrichment, as the decline of these species was observed in the combined treatment (containing nitrate) as well as nitrate on its own (Fig. 4B and C). Ammonium treatment alone did not influence any single taxon significantly in either direction.

These results were corroborated by models produced using the R package 'corncob,' which modeled relative abundance of individual taxa using beta-binomial regression models while accounting for variation in sequencing depth (Martin et al. 2020). Differential abundance was modeled as a function of (1) nutrient type, (2) nutrient concentration, and (3) nutrient exposure weeks. While some minor taxa responded negatively to nutrient treatment, the genus *Aquarickettsia* responded positively (Figures S9, S10, and Table S7, Supporting Information). No taxa were identified as significantly differentially abundant between high and low treatment concentrations The expected relative abundance of *Aquarickettsia* was modeled by nutrient and nutrient exposure weeks (Table S7, Supporting Information). While all nutrient treatments had a positive coefficient compared to T0 (indicating a significant positive response of *Aquarickettsia* to treatment; Figure S9, Supporting Information), 3 weeks of phosphate treatment had the strongest effect on relative abundance of *Aquarickettsia*, followed by 6 weeks of phosphate treatment. The combined treatment induced the next strongest response, while treatment with nitrate induced the smallest change in *Aquarickettsia* relative abundance

(though still significant compared to T0; Table S7, Supporting Information). When the effect of nutrient exposure weeks was examined on variability of *Aquarickettsia* populations between samples (dispersion of this taxon), both 3 and 6 weeks of exposure to phosphate were found to significantly decrease dispersion, as was 6 weeks of treatment with combined nutrients. No other treatments had a significant impact on dispersion (Table S7, Supporting Information).

Nutrient enrichment depressed growth rates but increased visual symbiont density

Net TLE was measured in millimeters from fragments sampled at 3 and 6 weeks of treatment (97 corals total, Fig. 5). Corals exposed to no treatment had the highest growth rates overall (13.33 ± 1.15 mm by 6 weeks, $n = 6$) with corals exposed to all other treatments exhibiting lower growth rates. Exposure to high levels (4x ambient) of combined treatment resulted in the lowest amount of TLE (4.40 ± 2.61 mm by 6 weeks, $n = 9$), with both low and high levels of combined treatment reducing growth rates significantly by only 3 weeks compared to untreated corals ($P < .05$, Tukey's pairwise honest significance test on log-transformed data. Table S8, Supporting Information). Both low and high levels of phosphate treatment led to significantly reduced TLE compared to untreated corals by 3 weeks of exposure (Table S8, Supporting Information). While not significant at $\alpha = 0.05$, 3 weeks of nitrate treatment led to a trend in reduced growth rates compared to untreated corals with $P = .058$ (LN) and $P = .068$ (HN). By 6 weeks of exposure, TLE was variable such that only high combined-treated corals had significantly lower growth rates compared to untreated corals. Algal symbiont density was assessed using a standardized color reference card (CoralWatch Coral Health Chart, Siebeck et al. 2008). T0 corals ($n = 53$) were deemed visually healthy after a week of acclimation to tank conditions (health score 4.92 ± 0.448), but rather than paling over the course of nutrient exposure, symbiont densities responded positively to tank conditions (Figure S11, Supporting Information, health score 5.88 ± 0.331 by week six, $n = 59$). All corals exhibited increases in symbiont density and differences by treatment were found to be insignificant ($P > .05$, Kruskal–Wallis test with Benjamini–Hochberg correction), although average health scores for untreated corals at 6 weeks (5.71 ± 0.469, $n = 6$) were lower than for nutrient-enriched corals (5.96 ± 0.191, $n = 53$).

Discussion

Aquarickettsia rohweri dominates the microbiome of disease-susceptible *A. cervicornis* genotypes

Numerous studies have demonstrated the surprising dominance of the parasitic genus *Aquarickettsia* in microbiomes of *A. cervicornis*, and in particular, of disease-susceptible genets of this species (Shaver et al. 2017, Rosales et al. 2019, Klinges et al. 2020, Baker et al. 2021, Aguirre et al. 2022, Miller et al. 2020, Casas et al. 2004, Gignoux-Wolfsohn et al. 2020). Results from this study were consistent with previous work, as populations of *Aquarickettsia* were found to comprise 74.98% of the microbiome in samples of *A. cervicornis* genotype 50, a disease-susceptible genotype (Muller et al. 2018). We previously showed that disease-resistant genotypes of *A. cervicornis*, in contrast to disease-susceptible genotypes, are characterized by a diverse, even microbiome with no single member exceeding 11% relative abundance (Klinges et al. 2020). Several studies suggest that high microbial diversity provides the host with greater defense resources to combat microbial invaders (Bourne et al. 2016, West et al. 2019) and that exposure to many
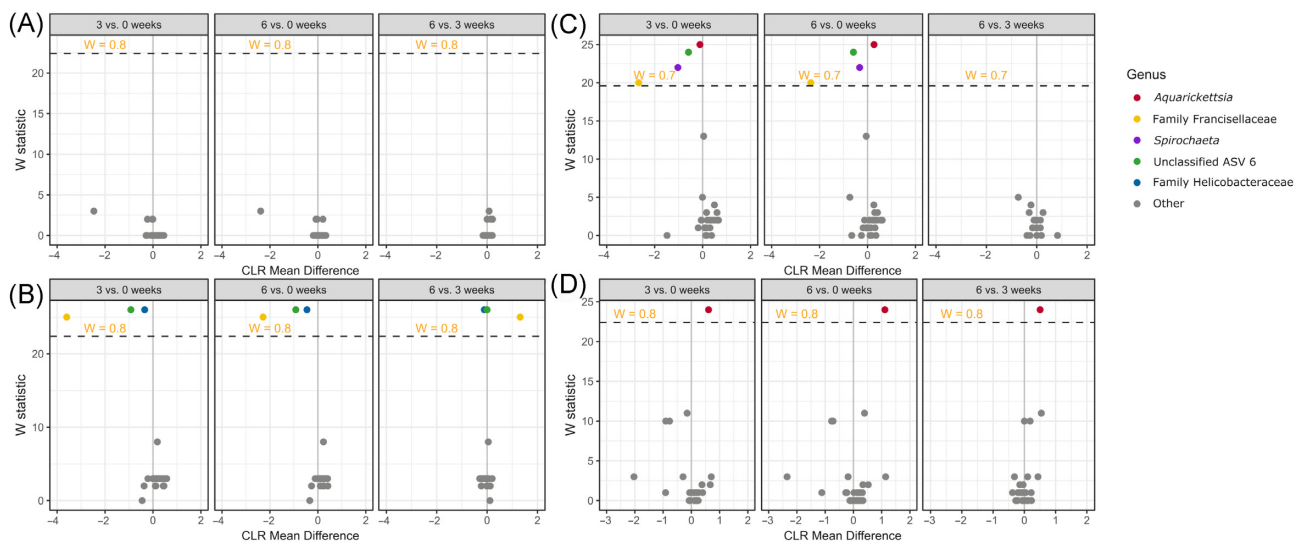
Figure 4. Volcano plots of results from differential abundance analysis with ANCOM-II by individual nutrient treatment. **(A)**. Ammonium **(B)**. Nitrate **(C)**. Combined **(D)**. Phosphate. Analysis performed on genus-level ASV table was filtered to include taxa with a total count of 10 in at least 20% of samples (ntaxa = 29) was used. ANCOM tests the null-hypothesis that the average abundance of a given species in a group is equal to that in the other group. Contrasts were performed as subsets of each individual treatment from full ASV table. The W statistic represents the strength of the test for the 29 tested species and is the number of times the null-hypothesis was rejected for a given species. Taxa above the dashed line are significant with the null-hypothesis rejected 80% of the time (W = 0.8), or 70% of the time for combined treatment samples (W = 0.7). Nonsignificant taxa in any contrast are colored grey. The x-axis value presents the effect size as the CLR-transformed mean difference in abundance of a given species between the two groups being compared.
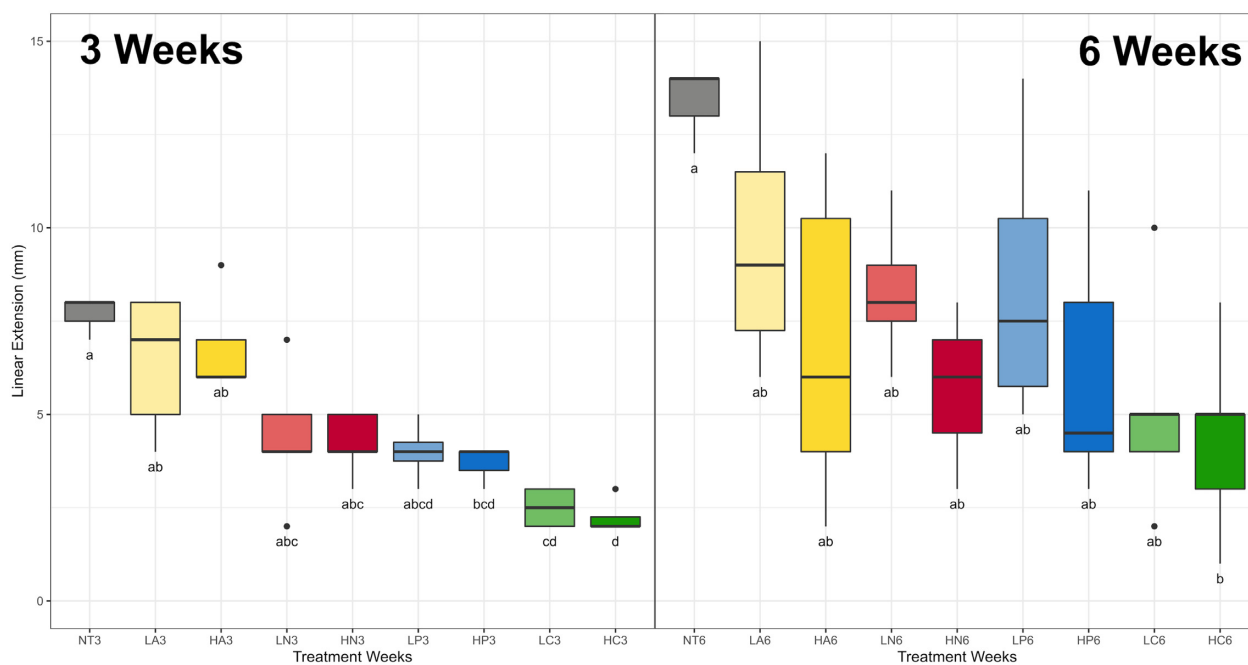
Figure 5. TLE calculated from measurements taken at 0, 3, and 6 weeks of nutrient exposure. Tukey's honest significance test was used on log-transformed data to identify significant differences in mean TLE by nutrient treatment and exposure weeks. Untransformed data is plotted for clarity. Boxes sharing a letter are not significantly different from each other using a significance level of $P < .05$.

different bacterial taxa increases host plasticity and ability to respond to changing environmental conditions (West et al. 2019; Zilber-Rosenberg and Rosenberg 2008). Voolstra and Ziegler (2020) argue that the microbiome flexibility and diversity in many *Acropora* species contributes to their ability to acclimate and adapt to environmental stressors, while leaving them more vulnerable to disease. They theorized that peak ecological capacity could be reached if genera with high physiological plasticity reach higher

microbiome flexibility, by means of probiotics or genetic engineering. In contrast, if a coral known to lack high physiological plasticity were to lose microbiome flexibility, adaptability to stressors would be reduced even further. The consistent dominance of *Aquarickettsia* in all recently sequenced samples of *A. cervicornis* is concerning, as some studies have shown that the overabundance of a single taxon may result in the destabilization of the remaining bacterial community through effects on host immunity (reviewed

in Rooks and Garrett 2016, and Hooper et al. 2012), further reducing the potential for adaptability in these corals.

Impacts of nutrient enrichment on coral physiology and microbiome structure

Nutrient enrichment alters the coral microbiome primarily through increases in opportunistic species that may contribute to disease (Thompson et al. 2015, Zaneveld et al. 2016, Shaver et al. 2017, Wang et al. 2018). While nutrient enrichment alone does not often induce mortality, the interaction of enrichment with other stressors such as thermal stress and loss of herbivorous fish species has been demonstrated to prolong bleaching and increase coral mortality (Zaneveld et al. 2016, Wang et al. 2018). Anthropogenic nutrification of oligotrophic reefs often leads to not only an increase in the primary constituents of terrestrial runoff (ammonium, nitrate, and phosphate) but also an alteration of the ratio between their concentrations (Brodie et al. 2011, Wiedenmann et al. 2013). While anthropogenic pollution tends to deliver more nitrate, ammonium is primarily derived from fish excretion (Allgeier et al. 2017). As such, we investigated the impacts of increased levels of each constituent on microbial community composition and coral health. While nitrogen enrichment leads to the proliferation of the coral algal symbiont Symbiodiniaceae (Muscatine et al. 1989, Cunning and Baker 2013) phosphate alone does not affect symbiont density. We nonetheless found that symbiont density (as measured visually by changes in coral color) increased across all treatments in this experiment. Nitrate enrichment has been hypothesized to affect the translocation of nutrients between Symbiodiniaceae and the coral host (Shantz and Burkepile 2014, Shantz et al. 2016), and it has been suggested that the host controls symbiont density through nitrogen and phosphorus limitation to maximize carbon return from this symbiosis (Wooldridge 2010). Further, overabundance of dissolved inorganic nitrogen leads to phosphate limitation in corals as a result of algal proliferation, causing increased susceptibility to light- and temperature-induced bleaching (Wiedenmann et al. 2013, Rosset et al. 2017). Nitrate has been demonstrated to decrease coral growth rates, while ammonium did not (Shantz and Burkepile 2014). Excess phosphate, in contrast to nitrate, has minimal impact on coral physiology and may increase stress tolerance (Wiedenmann et al. 2013, Shantz and Burkepile 2014). In fact, during thermal stress, phosphate uptake is increased in order to maintain symbiont density and carbon translocation (Ezzat et al. 2016). Ammonium, which is often naturally derived in reef systems from fish excretion, may enhance coral growth (reviewed in Shantz and Burkepile 2014).

In light of these data, we hypothesized that nitrate enrichment would lead to the lowest coral growth rates over the course of enrichment and would lead to the greatest impact on microbiome structure. While nitrate treatment led to a trend of decreased coral growth rates, only exposure to the combination treatment (including nitrate, phosphate, and ammonium) significantly reduced coral growth rates compared to untreated samples. The addition of nitrate led to the significant decrease in minor taxa, but not to significant changes in *Aquarickettsia*. Phosphate treatment was the driving nutrient constituent in shifts of *Aquarickettsia*, with corals exposed to a combined treatment containing phosphate also exhibiting shifts in this taxon (Fig. 4C and D). Treatment with ammonium did not significantly impact any individual microbial taxon (Fig. 4A), nor did it significantly impact growth rates, consistent with the minimal effects observed from frequent, low-level introduction of ammonium to reef environments in the form

of fish excretion (Shantz and Burkepile 2014, Rice et al. 2019). Differences in alpha and beta diversity and in relative and absolute abundance of *Aquarickettsia* between 3 and 6 weeks of nutrient exposure were largely insignificant across all conditions. Importantly, this suggests that 3 weeks of exposure to tank conditions or nutrient treatment was sufficient to shift microbiomes to a new stable state.

Phosphate enrichment shifted microbial populations further towards dysbiosis

Phosphate and combined nutrient treatments led to a decrease in community dispersion by only 3 weeks of exposure (Figure S6, Supporting Information), and removal of *Aquarickettsia* from the dataset erased this effect (Figure S7, Supporting Information), suggesting that significant increases in *Aquarickettsia* were the driver of these shifts in community composition. While the addition of environmental stressors has been found to increase community dispersion in other studies (Zaneveld et al. 2017; Maher et al. 2019; Klinges et al. 2020), we found that dispersion generally decreased over the course of nutrient exposure. Zaneveld et al. (2017) posited that increases in dispersion resulting from stress are suggestive of microbiome instability resulting from stochastic shifts differing by individual. We argue that the trends observed in this study represent a takeover by an opportunistic species that excludes beneficial members from the microbiome, resulting in a different form of microbiome instability. Though dispersion decreased overall with enrichment, we found the magnitude of observed increase in the dominant constituent of *A. cervicornis* microbiomes differed by nutrient constituent. Differential abundance analyses revealed that abundance of *Aquarickettsia* was significantly altered in phosphate and combined treatments. Corals exposed to combined treatment demonstrated decreased growth rates over the course of the experiment, consistent with the hypothesized parasitism of essential host metabolites by *Aquarickettsia*. As decreases in growth rate as well as microbial community shifts were largely insignificant for ammonium and nitrate treatments, the majority of the response to combined nutrient treatment can be attributed to the phosphate in this treatment. This microbial response to phosphate and combination nutrient enrichment is consistent with our previous predictions of *Aquarickettsia* life strategy, namely, that *Aquarickettsia* is a parasite, dependent on nutritional supplementation from the algal symbiont (Klinges et al. 2019), and responds positively to nutrient enrichment (Shaver et al. 2017). As algal symbiont density was visually observed to increase over the course of experimentation, it is likely that *Aquarickettsia* utilized surplus amino acids and sugars produced by elevated symbiont populations.

We previously identified annotations for a complete PhoR–PhoB two component system in the genome of *A. rohweri* (Klinges et al. 2019). This system, notably absent in the genomes of closely related species in the order Rickettsiales, allows for sensing of extracellular inorganic phosphate concentrations. Paired with evidence that phosphate stimulates abundance of *Aquarickettsia*, it is likely that the PhoR–PhoB system plays a role in cellular proliferation or upregulation of virulence factors in this species. The Pho regulon has been found to modulate the expression of genes involved in survival response (*via* production of poly P, ppGpp, and RpoS), virulence, motility, and biofilm formation through quorum sensing in various strains of pathogenic bacteria (Lamarche et al. 2008). The transcriptional-response regulator PhoB translates signals of phosphate depletion or enrichment into gene activation or repression. Recently, the histidine kinase PhoR was previously

found to be involved in the upregulation of swarming, flagellar motility, and T3SS expression in the pathogen *Vibrio parahaemolyticus* (Zhang et al. 2020). Control of gene activity by this regulon has been suggested to play a role in life strategy in bacteria experiencing large shifts in phosphate levels, leading to a switch between a motile swimming phase and a biofilm-forming or intracellular phase. *Aquarickettsia* encodes a nearly complete flagellar assembly and no evidence has been found of vertical transmission of this species, suggesting it may have a brief free-living life stage (Baker et al. 2021). It is, therefore, possible that high phosphate levels act as a cue for upregulation of virulence and host cell infiltration, as well as increased cell replication due to an abundance of phosphate for the production of nucleic acids.

Multiple measures of *Aquarickettsia* abundance elucidate its dynamics in response to nutrient enrichment

Regardless of nutrient constituent or concentration, the absolute abundance of the putative bacterial parasite *Aquarickettsia* increased with time. This trend also included untreated samples, confounding an association of *Aquarickettsia* populations with nutrient type. Although examination of *Aquarickettsia* relative abundance over the course of experimentation indicated that phosphate treatment induced the greatest shift in *Aquarickettsia* abundance, analyses of differential abundance of this taxon were also performed due to known issues with relative abundance data. Relative abundance metrics are easily confounded by shifts in one taxonomic group—even if the absolute abundance of most taxa remains unchanged, increases in one taxon will deflate the relative abundance of other taxa (Mandal et al. 2015, Gloor et al. 2017). Differential abundance analysis confirmed that shifts in *Aquarickettsia* relative to other taxa were not significant in any nutrient treatment besides phosphate or combined treatments. Differential abundance tools such as ANCOM-II and corncob may reflect more accurately shifts in individual taxa, as they account for the inherent issues with compositional data, including excess zeroes, though each of these tools utilizes a slightly different method to identify differentially abundant taxa.

While total bacterial abundance was not quantified in this study, the inconsistencies between differential abundance data and absolute abundance data suggest that an increase in total bacterial abundance occurred throughout the course of the experiment, such that absolute abundance of *Aquarickettsia* increased in untreated, nitrate, and ammonium-treated samples, but proportions of this taxon compared to other species did not change significantly. This increase in total bacterial abundance may be attributed to the elevated nutrient levels across all treatments, as the nearshore water used in this study was found to have higher levels of nitrate than Mote's nursery near Looe Key Reef (Lapointe et al. 2019) from which coral fragments were sourced (Figure S1, Supporting Information), though phosphate and ammonium levels were comparable. Thus, while nitrate levels were elevated ~4-fold significantly compared to Looe Key reef conditions in all samples, phosphate levels were only enriched compared to reef conditions in phosphate-treated or combination-treated samples. It is therefore possible that we did not capture the true response of these corals to nitrate enrichment, as they had been allowed to acclimate to high-nutrient conditions prior to experimental manipulation. While Looe Key Reef is not truly oligotrophic (Lapointe et al. 2019), it is possible that the transplant of these coral individuals from a nutrient-limited system to a nutrient-rich system stimulated a bacterial bloom in all samples. Nutrient enrichment

has been demonstrated to lead to increased algal growth, leading to the increased production of algal exudates. These exudates are high in dissolved sugars, which rapidly stimulate bacterial growth (Nelson et al. 2013, Bourne et al. 2016). The observed bacterial bloom appeared to affect all bacterial taxa indiscriminately, as differential abundance analysis found no taxa were significantly enriched or depleted in untreated samples after 6 weeks of exposure to tank conditions in comparison to T0. While previous work in Mediterranean coastal oligotrophic waters found that bacterial biomass responded most dramatically to increases in total nutrient concentrations (Sipura et al. 2005, Rahav et al. 2018), studies performed in the Florida Bay indicated that this system was highly phosphate-limited due to excess nitrogen and carbon inputs (Fourqurean et al. 1993, Cotner et al. 2000). It is, thus surprising that overall bacterial abundance appeared to increase in response to the nitrate-enriched, but not phosphate-enriched, conditions in unamended aquarium water, though no single taxon shifted significantly in respect to other taxa.

Conclusions

Nutrient enrichment significantly effects coral microbiome dysbiosis and increases disease susceptibility, though the effects of individual nutrient constituents and shifts in N:P ratios remain under-characterized. Previous work has demonstrated a positive response of the parasitic genus *Aquarickettsia* to a combined nutrient treatment with corresponding negative effects on coral growth rates (Shaver et al. 2017). Results of the present study, however, suggest that *Aquarickettsia* responds most significantly to phosphate enrichment. Microbial diversity decreased over the course of nutrient enrichment in phosphate- and combined-treated samples, reflective of increased dominance of *Aquarickettsia*, and differential abundance of *Aquarickettsia* was only significant in these treatments. Fragment linear extension after 6 weeks of exposure to these treatments was also significantly lower than in other treatments. Alpha diversity decreased in nitrate-treated samples as a result of a significant decline in minor taxa. While results from quantitative PCR showed an increase in *Aquarickettsia* across all samples throughout the course of experimentation, significant shifts in individual taxa were not observed in ammonium-treated and untreated samples. This suggests that an increase in total bacterial abundance occurred in all samples, but only amendment with phosphate was sufficient to alter dominance of the predicted parasite *Aquarickettsia* over other bacterial species.

Supplementary data

Supplementary data are available at *FEMSEC* online.

Data availability statement

Raw sequence data were deposited into the NCBI Sequence Read Archive (SRA) under accession BioProject PRJNA756691. All scripts involved in the preparation and analysis of this dataset are available at https://github.com/graceklinges/disease-susceptible-micro.

Authors' contributions

J.G.K., R.V.T., and E.M.M. designed the nutrient enrichment experiment, J.G.K. and W.D. performed the experiment, J.G.K. and S.P. analyzed the data, J.G.K. wrote the manuscript, and all authors contributed to data interpretation and editing of the manuscript.

Acknowledgments

Funding

References

Aguirre EG, Million WC, Bartels E *et al*. Host-specific epibiomes of distinct *Acropora cervicornis* genotypes persist after field transplantation. *Coral Reefs* 2022. DOI: 10.1007/s00338-022-02218-x. https://link.springer.com/article/10.1007/s00338-022-02218-x.

Allgeier JE, Burkepile DE, Layman CA. Animal pee in the sea: consumer-mediated nutrient dynamics in the world's changing oceans. *Glob Change Biol* 2017;**23**:2166–78.

Anderson MJ. A new method for non-parametric multivariate analysis of variance. *Austral Ecol* 2001;**26**:32–46.

Anderson MJ. Distance-based tests for homogeneity of multivariate dispersions. *Biometrics* 2006;**62**:245–53.

Apprill A, McNally S, Parsons R *et al*. Minor revision to V4 region SSU rRNA 806R gene primer greatly increases detection of SAR11 bacterioplankton. *Aquat Microb Ecol* 2015;**75**:129–37.

Baker LJ, Reich HG, Kitchen SA *et al*. The coral symbiont *Candidatus Aquarickettsia* is variably abundant in threatened Caribbean acroporids and transmitted horizontally. *ISME J* 2021; **16**:400–11. DOI: 10.1038/s41396-021-01077-8.

Benjamini Y, Hochberg Y. Controlling the false discovery rate: a practical and powerful approach to multiple testing. *J R Stat Soc Series B Stat Methodol* 1995;**57**:289–300.

Bennett EM, Carpenter SR, Caraco NF. Human impact on erodable phosphorus and eutrophication: a global perspective: increasing accumulation of phosphorus in soil threatens rivers, lakes, and coastal oceans with eutrophication. *Bioscience* 2001;**51**:227–34.

Bourne D, Iida Y, Uthicke S *et al*. Changes in coral-associated microbial communities during a bleaching event. *ISME J* 2008;**2**:350–63.

Bourne DG, Morrow KM, Webster NS. Insights into the coral microbiome: underpinning the health and resilience of reef ecosystems. *Annu Rev Microbiol* 2016;**70**:317–40.

Brodie JE, Devlin M, Haynes D *et al*. Assessment of the eutrophication status of the Great Barrier Reef lagoon (Australia). *Biogeochemistry* 2011;**106**:281–302.

Bruno JE, Petes LE, Harvell CD *et al*. Nutrient enrichment can increase the severity of coral diseases. *Ecol Lett* 2003;**6**:1056–61. DOI: 10.1046/j.1461-0248.2003.00544.x .

Callahan BJ, McMurdie PJ, Rosen MJ *et al*. DADA2: high-resolution sample inference from Illumina amplicon data. *Nat Methods* 2016;**13**:581–3.

Casas V, Kline DI, Wegley L *et al*. Widespread association of a Rickettsiales-like bacterium with reef-building corals. *Environ Microbiol* 2004;**6**:1137–48.

Cotner JB, Sada RH, Bootsma H *et al*. Nutrient limitation of heterotrophic bacteria in Florida Bay. *Estuaries* 2000;**23**:611–20.

Cunning R, Baker AC. Excess algal symbionts increase the susceptibility of reef corals to bleaching. *Nat Clim Change* 2013;**3**:259–62.

De'ath G, Fabricius K. Water quality as a regional driver of coral biodiversity and macroalgae on the Great Barrier Reef. *Ecol Appl* 2010;**20**:840–50.

Donovan MK, Burkepile DE, Kratochwill C *et al*. Local conditions magnify coral loss after marine heatwaves. *Science* 2021;**372**:977–80.

Ezzat L, Merolla S, Clements CS *et al*. Thermal Stress Interacts With Surgeonfish Feces to Increase Coral Susceptibility to Dysbiosis and Reduce Tissue Regeneration *Front microbiol* 2021;**12**:e620458.

Ezzat L, Towle E, Irisson J-O *et al*. The relationship between heterotrophic feeding and inorganic nutrient availability in the scleractinian coral *T. reniformis* under a short-term temperature increase. *Limnol Oceanogr* 2016;**61**:89–102.

Fourqurean JW, Jones RD, Zieman JC. Process influencing water column nutrient characteristics and phosphorus limitation of phytoplankton biomass in Florida Bay, FL, USA: inferences from spatial distributions. *Estuar Coast Shelf Sci* 1993;**36**:295–314.

Gignoux-Wolfsohn S, Precht W, Peters E *et al*. Ecology, histopathology, and microbial ecology of a white-band disease outbreak in the threatened staghorn coral *Acropora cervicornis*. *Dis Aquat Organ* 2020;**137**:217–37.

Glasl B, Herndl GJ, Frade PR. The microbiome of coral surface mucus has a key role in mediating holobiont health and survival upon disturbance. *ISME J* 2016;**10**:2280–92.

Gloor GB, Macklaim JM, Pawlowsky-Glahn V *et al*. Microbiome datasets are compositional: and this is not optional. *Front Microbiol* 2017;**8**: 2224. DOI: 10.3389/fmicb.2017.02224.

Heip CHR, Herman PMJ, Soetaert K. Indices of diversity and evenness. *Océanis* 2001;**24**:61–87.

Hooper LV, Littman DR, Macpherson AJ. Interactions between the microbiota and the immune system. *Science* 2012;**336**:1268–73.

Huang D, Roy K. The future of evolutionary diversity in reef corals. *Philos Trans R Soc B Biol Sci* 2015;**370**:20140010.

Hughes TP, Kerry JT, Álvarez-Noriega M *et al*. Global warming and recurrent mass bleaching of corals. *Nature* 2017;**543**:373–7.

Jian C, Luukkonen P, Yki-Järvinen H et al. Quantitative PCR provides a simple and accessible method for quantitative microbiota profiling. *PLOS ONE* 2020;**15**:e0227285. DOI: 10.1371/journal.pone.0227285.

Kaul A, Mandal S, Davidov O *et al*. Analysis of microbiome data in the presence of excess zeros. *Front Microbiol* 2017;**8**:2114. DOI: 10.3389/fmicb.2017.02114.

Klinges G, Maher RL, Thurber RLV *et al*. Parasitic 'Candidatus Aquarickettsia rohweri' is a marker of disease susceptibility in *Acropora cervicornis* but is lost during thermal stress. *Environ Microbiol* 2020;**22**:5341–55.

Klinges JG, Rosales SM, McMinds R *et al*. Phylogenetic, genomic, and biogeographic characterization of a novel and ubiquitous marine invertebrate-associated *Rickettsiales* parasite, *Candidatus Aquarickettsia rohweri*, gen. nov., sp. nov. *ISME J* 2019;**13**:2938–53.

Krediet CJ, Ritchie KB, Paul VJ *et al*. Coral-associated micro-organisms and their roles in promoting coral health and thwarting diseases. *Proc Biol Sci* 2013;**280**:20122328. DOI: 10.1098/rspb.2012.2328.

Lahti L, Shetty S. "microbiome R package". 2012. http://microbiome.github.io/.

Lamarche MG, Wanner BL, Crépin S *et al*. The phosphate regulon and bacterial virulence: a regulatory network connecting phos-

phate homeostasis and pathogenesis. *FEMS Microbiol Rev* 2008;**32**: 461–73.

Lapointe BE, Bedford BJ. Stormwater nutrient inputs favor growth of non-native macroalgae (Rhodophyta) on O'ahu, Hawaiian Islands. *Harmful Algae* 2011;**10**:310–8.

Lapointe BE, Brewton RA, Herren LW *et al.* Nitrogen enrichment, altered stoichiometry, and coral reef decline at Looe Key, Florida Keys, USA: a 3-decade study. *Mar Biol* 2019;**166**:108.

Liu L, Salam N, Jiao J-Y *et al. Cysteiniphilum litorale* gen. nov., sp. nov., isolated from coastal seawater. *Int J Syst Evol Microbiol* 2017;**67**:2178–83.

Maher RL, Rice MM, McMinds R et al. Multiple stressors interact primarily through antagonism to drive changes in the coral microbiome. *Sci Rep* 2019;**9**:1–12. DOI: 10.1038/s41598-019-43274-8.

Maher RL, Schmeltzer ER, Meiling S *et al.* Coral microbiomes demonstrate flexibility and resilience through a reduction in community diversity following a thermal stress event. *Front Ecol Evol* 2020;**8**: 555698. DOI: 10.3389/fevo.2020.555698.

Mandal S, Van Treuren W, White RA *et al.* Analysis of composition of microbiomes: a novel method for studying microbial composition. *Microb Ecol Health Dis* 2015;**26**:27663. DOI: 10.3402/mehd.v26.27663.

Martin BD, Witten D, Willis AD. Modeling microbial abundances and dysbiosis with beta-binomial regression. *Ann App Stat* 2020;**14**: 94–115.

Martin M. Cutadapt removes adapter sequences from high-throughput sequencing reads. *EMBnet J* 2011;**17**:10–2.

Martinez Arbizu P. pairwiseAdonis: pairwise multilevel comparison using adonis. *R package version 001* 2017. https://github.com/pmartinezarbizu/pairwiseAdonis.

McDevitt-Irwin JM, Baum JK, Garren M *et al.* Responses of coral-associated bacterial communities to local and global stressors. *Front Mar Sci* 2017;**4**: 262. DOI: 10.3389/fmars.2017.00262.

McMurdie PJ, Holmes S. phyloseq: an R package for reproducible interactive analysis and graphics of microbiome census data. *PLoS ONE* 2013;**8**:e61217. Watson M (ed.).

Messyasz A, Maher RL, Meiling SS *et al.* Nutrient enrichment predominantly affects low diversity microbiomes in a marine trophic symbiosis between algal farming fish and corals. *Microorganisms* 2021;**9**:1873.

Miller MW, Lohr KE, Cameron CM *et al.* Disease dynamics and potential mitigation among restored and wild staghorn coral, *Acropora cervicornis. PeerJ* 2014;**2**:e541.

Miller N, Maneval P, Manfrino C *et al.* Spatial distribution of microbial communities among colonies and genotypes in nursery-reared *Acropora cervicornis. PeerJ* 2020;**8**:e9635.

Muller EM, Bartels E, Baums IB. Bleaching causes loss of disease resistance within the threatened coral species *Acropora cervicornis.Elife* 2018;**7**: e35066. DOI: 10.7554/eLife.35066.

Muscatine L, Falkowski PG, Dubinsky Z *et al.* The effect of external nutrient resources on the population dynamics of zooxanthellae in a reef coral. *Proc R Soc Lond B* 1989;**236**:311–24.

Nelson CE, Goldberg SJ, Wegley Kelly L *et al.* Coral and macroalgal exudates vary in neutral sugar composition and differentially enrich reef bacterioplankton lineages. *ISME J* 2013;**7**:962–79.

Oksanen J, Blanchet FG, Friendly M *et al.* Vegan: community ecology package. 2019. https://cran.r-project.org/web/packages/vegan/index.html.

Pachiadaki MG, Kallionaki A, Dählmann A *et al.* Diversity and spatial distribution of prokaryotic communities along a sediment vertical profile of a deep-sea mud volcano. *Microb Ecol* 2011;**62**:655–68.

Pantos O, Cooney RP, Tissier MDAL *et al.* The bacterial ecology of a plague-like disease affecting the Caribbean coral *Montastrea annularis. Environ Microbiol* 2003;**5**:370–82.

Parada AE, Needham DM, Fuhrman JA. Every base matters: assessing small subunit rRNA primers for marine microbiomes with mock communities, time series and global field samples. *Environ Microbiol* 2016;**18**:1403–14.

Parkinson JE, Bartels E, Devlin-Durante MK *et al.* Extensive transcriptional variation poses a challenge to thermal stress biomarker development for endangered corals. *Mol Ecol* 2018;**27**:1103–19.

Pawlik JR, Burkepile DE, Thurber RV. A vicious circle? Altered carbon and nutrient cycling may explain the low resilience of Caribbean coral reefs. *Bioscience* 2016;**66**:470–6.

Peters E, Oprandy JJ, Yevich PP. Possible causal agent of "White Band Disease" in Caribbean Acroporid corals. *J Invertebr Pathol* 1983;**41**:394–6.

Pratte ZA, Longo GO, Burns AS *et al.* Contact with turf algae alters the coral microbiome: contact versus systemic impacts. *Coral Reefs* 2018;**37**:1–13.

Quast C, Pruesse E, Yilmaz P *et al.* The SILVA ribosomal RNA gene database project: improved data processing and web-based tools. *Nucleic Acids Res* 2012;**41**:D590–6.

R Core Team. R: A language and environment for statistical computing. Vienna, Austria: R Foundation for Statistical Computing, 2019. https://www.R-project.org/.

Rahav E, Raveh O, Hazan O *et al.* Impact of nutrient enrichment on productivity of coastal water along the SE Mediterranean shore of Israel - a bioassay approach. *Mar Pollut Bull* 2018;**127**: 559–67.

Rice MM, Maher RL, Thurber RV *et al.* Different nitrogen sources speed recovery from corallivory and uniquely alter the microbiome of a reef-building coral. *PeerJ* 2019;**7**:e8056.

Rooks MG, Garrett WS. Gut microbiota, metabolites and host immunity. *Nat Rev Immunol* 2016;**16**:341–52.

Rosales SM, Miller MW, Williams DE *et al.* Microbiome differences in disease-resistant vs. susceptible Acropora corals subjected to disease challenge assays. *Sci Rep* 2019;**9**:18279.

Rosenberg E, Koren O, Reshef L *et al.* The role of microorganisms in coral health, disease and evolution. *Nat Rev Microbiol* 2007;**5**: 355–62.

Rosset S, Wiedenmann J, Reed AJ *et al.* Phosphate deficiency promotes coral bleaching and is reflected by the ultrastructure of symbiotic dinoflagellates. *Mar Pollut Bull* 2017;**118**:180–7.

Shantz AA, Burkepile DE. Context-dependent effects of nutrient loading on the coral–algal mutualism. *Ecology* 2014;**95**:1995–2005.

Shantz AA, Lemoine NP, Burkepile DE. Nutrient loading alters the performance of key nutrient exchange mutualisms. *Ecol Lett* 2016;**19**:20–8.

Shaver EC, Shantz AA, McMinds R *et al.* Effects of predation and nutrient enrichment on the success and microbiome of a foundational coral. *Ecology* 2017;**98**:830–9.

Siebeck UE, Logan D, Marshall NJ. CoralWatch – a flexible coral bleaching monitoring tool for you and your group. In: *Proceedings of the 11th International Coral Reef Symposium, Ft. Lauderdale, Florida, 7-11 July.* 2008. Session number 16, 1392: 5.

Sipura J, Haukka K, Helminen H *et al.* Effect of nutrient enrichment on bacterioplankton biomass and community composition in mesocosms in the Archipelago Sea, northern Baltic. *J Plankton Res* 2005;**27**:1261–72.

Sunagawa S, Woodley CM, Medina M. Threatened corals provide underexplored microbial habitats. *PLoS ONE* 2010;**5**:e9554.

Thompson JR, Rivera HE, Closek CJ *et al*. Microbes in the coral holobiont: partners through evolution, development, and ecological interactions. *Front Cell Infect Microbiol* 2015;**4**:176. DOI: 10.3389/fcimb.2014.00176.

Thurber RV, Burkepile DE, Correa AMS *et al*. Macroalgae decrease growth and alter microbial community structure of the reef-building coral, porites astreoides. *PLoS ONE* 2012;**7**: e44246.

Vega Thurber RL, Burkepile DE, Fuchs C *et al*. Chronic nutrient enrichment increases prevalence and severity of coral disease and bleaching. *Glob Change Biol* 2014;**20**:544–54.

Voolstra CR, Ziegler M. Adapting with microbial help: microbiome flexibility facilitates rapid responses to environmental change. *Bioessays* 2020;**42**:2000004.

Voss JD, Richardson LL. Nutrient enrichment enhances black band disease progression in corals. *Coral Reefs* 2006;**25**:569–76.

Wang L, Shantz AA, Payet JP *et al*. Corals and their microbiomes are differentially affected by exposure to elevated nutrients and a natural thermal anomaly. *Front Mar Sci* 2018;**5**:13. DOI: 10.3389/fmars.2018.00101.

Webster NS, Reusch TBH. Microbial contributions to the persistence of coral reefs. *ISME J* 2017;**11**:2167–74.

West AG, Waite DW, Deines P *et al*. The microbiome in threatened species conservation. *Biol Conserv* 2019;**229**:85–98.

Wiedenmann J, D'Angelo C, Smith EG *et al*. Nutrient enrichment can increase the susceptibility of reef corals to bleaching. *Nat Clim Change* 2013;**3**:160.

Wooldridge SA. Is the coral-algae symbiosis really 'mutually beneficial' for the partners? *Bioessays* 2010;**32**:615–25.

Wright RM, Strader M, Genuise HM *et al*. Effects of thermal stress on amount, composition, and antibacterial properties of coral mucus. *PeerJ* 2019;**7**:e6849. DOI: 10.7717/peerj.6849.

Zaneveld JR, Burkepile DE, Shantz AA *et al*. Overfishing and nutrient pollution interact with temperature to disrupt coral reefs down to microbial scales. *Nat Commun* 2016;**7**:11833.

Zaneveld JR, McMinds R, Thurber RV. Stress and stability: applying the Anna Karenina principle to animal microbiomes. *Nat Microbiol* 2017;**2**:17121.

Zhang Y, Liu H, Gu D *et al*. Transcriptomic analysis of PhoR reveals its role in regulation of swarming motility and T3SS expression in *Vibrio parahaemolyticus*. *Microbiol Res* 2020;**235**:126448.

Ziegler M, Grupstra CGB, Barreto MM *et al*. Coral bacterial community structure responds to environmental change in a host-specific manner. *Nat Commun* 2019;**10**:3092.

Zilber-Rosenberg I, Rosenberg E. Role of microorganisms in the evolution of animals and plants: the hologenome theory of evolution. *FEMS Microbiol Rev* 2008;**723**:723–35. DOI: 10.1111/j.1574-6976.2008.00123.x.